

Supplemental Dataset

Supplemental methods

Characterization of Vegfc-floxed allele

Vegfc^{fl/+} mice were crossed to E11a-Cre mice to drive germline recombination (*Vegfc*^{RC/+}).

Vegfc^{RC/+} mice were timed mated with *Vegfc*^{RC/+} mice, and embryos were harvested at E15.5.

Embryos were imaged immediately after harvest using the Olympus SZX16 microscope and DP72 camera using the cellSens software. Embryos were then fixed in 4% PFA overnight at 4 °C, dehydrated to 100% EtOH, paraffin embedded, and sectioned, as described previously²⁵.

Sections were subjected to hematoxylin and eosin (H&E) and/or immunohistochemical staining using antibodies against Prox1 (Abcam ab76696) and Lyve1 (R&D AF2125). Images were acquired with an Olympus BX53 microscope, Olympus DP80 camera, using x20 and x40 objectives and the cellSens software, and processed using ImageJ.

RNA isolation and RT-qPCR

RNA was isolated from tissues using TRIzol Reagent (Life Technologies), and reverse transcribed to cDNA using the high-Capacity cDNA Reverse Transcription Kit (Applied Biosystems 4368814). qPCR was performed using Power SYBR Green PCR Master Mix (Applied Biosystems 4367659), using QuantStudio 6 Flex Real-Time PCR system (Applied Biosystems). Relative gene expression was normalized to *Gapdh* levels and calculated using the ddCT method. qPCR primer sequences are as follows:

mVegfc Forward: 5'- CAGCCCACCCTCAATACC -3'

mVegfc Reverse: 5'- CTCCTTCCCCACATCTATACAC -3'

mGapdh Forward: 5'- CATGGCCTTCCGTGTTCTTA -3'

mGapdh Reverse: 5'- CCTGCTTCACCACCTTCTTGAT -3'

Primer sequences for generation of FLAG-tagged VEGFD construct

Forward: 5'- CCA TAC TCA ATT ATC AGC AGC TCC ATC CAG ATC CCT GAA G -3'

Reverse: 5'- CTT CAG GGA TCT GGA TGG AGC TGC TGA TAA TTG AGT ATG G -3'

Labeling of platelets in vivo and imaging of injury sites

Mice were injected intravenously via the tail vein with 100 uL of PE-Cy7 anti-CD41 antibody.

Mice were then anesthetized with isoflurane, and given either the skin injury or tail injury.

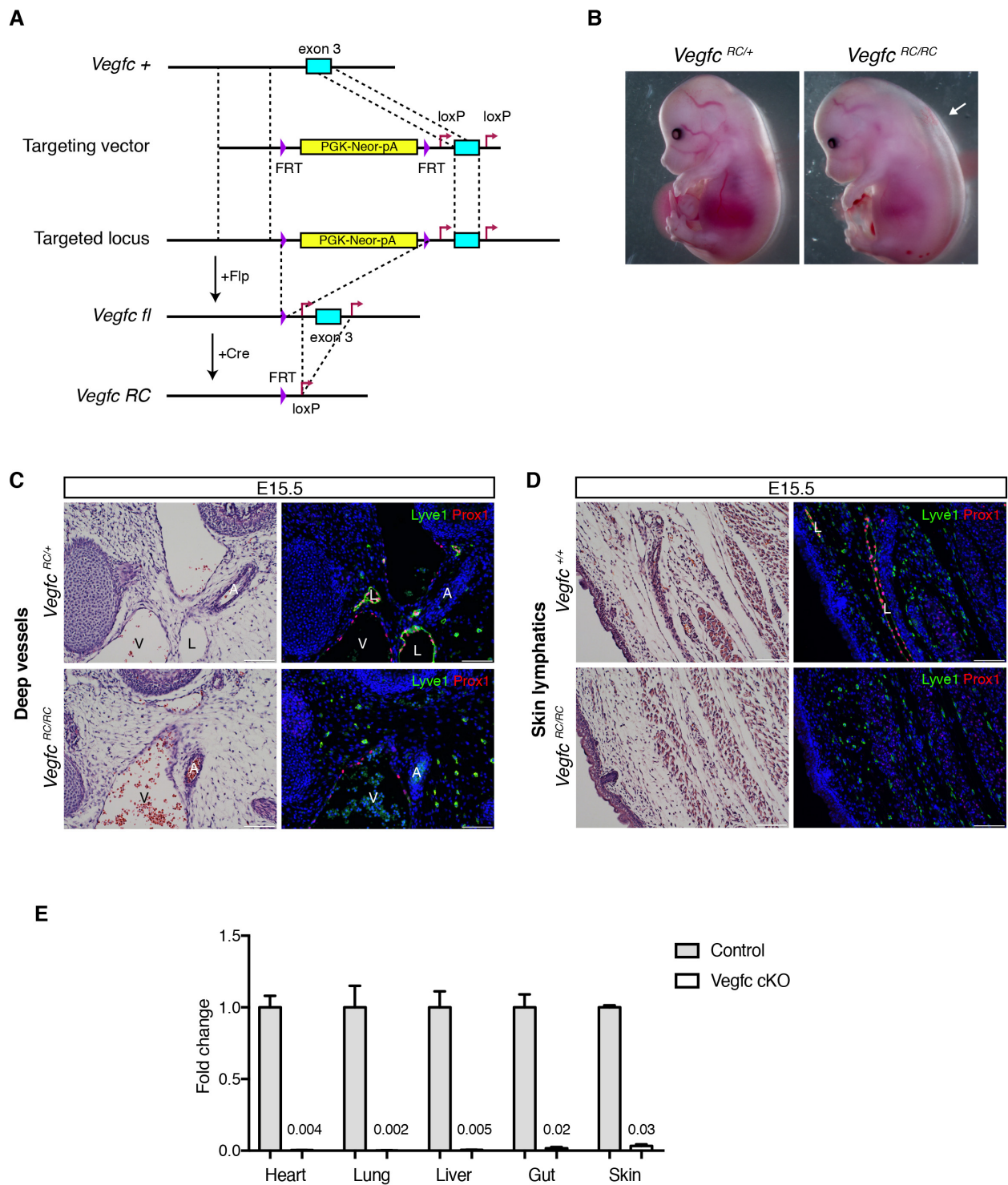
Immediately after injury, the wound site was imaged under the microscope in the bright field as well as red channels. The Olympus MVX10 microscope with an Olympus DP74 camera, and cellSens software were used for image acquisition, and Fiji used for image analysis. 3 mice were used for each injury.

Quantification of angiogenesis

Paraffin embedded wound tissues were stained with Pecam-1 antibody (HistoBioTech DIA-310).

To quantify angiogenesis, sections from the center, anterior, and posterior edges of the wound were chosen, and 1-4 random 20x fields were imaged for Pecam1 staining from each section, depending on the final size of the wound. The images were then thresholded on the Pecam-1 staining using the *Set Threshold* function in Fiji to select all Pecam-1 positive areas, and the area measured using the *Measure* function. % Pecam-1 positive area was defined as the total area positive for Pecam1 staining defined by the set threshold divided by the total area of a 20x field. Each point on the graph corresponds to the average % Pecam-1 positive area of all 20x fields imaged from one animal.

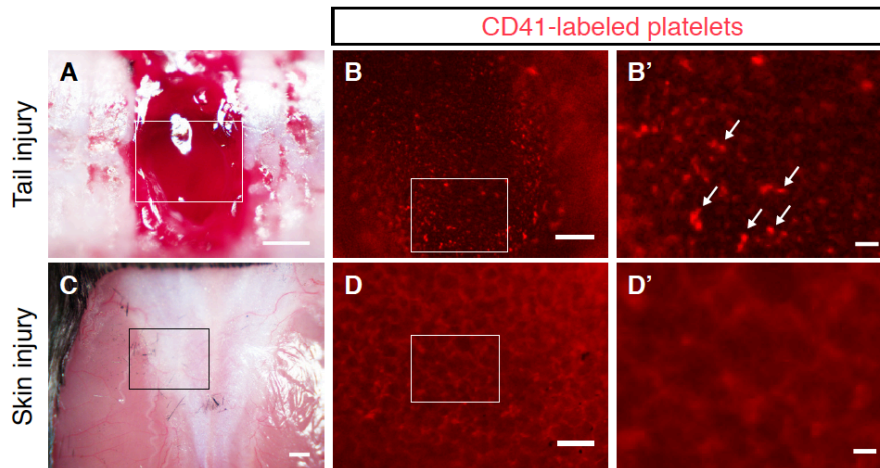
Supplemental figure 1



Supplemental Figure 1. Design and characterization of the *Vegfc*^{fl} allele. (A) Schematic of the targeted *Vegfc* allele. *Flp*-mediated recombination drives excision of the Neomycin-resistance cassette to generate the floxed allele (*Vegfc*^{fl}) used in these studies. *Cre*-mediated

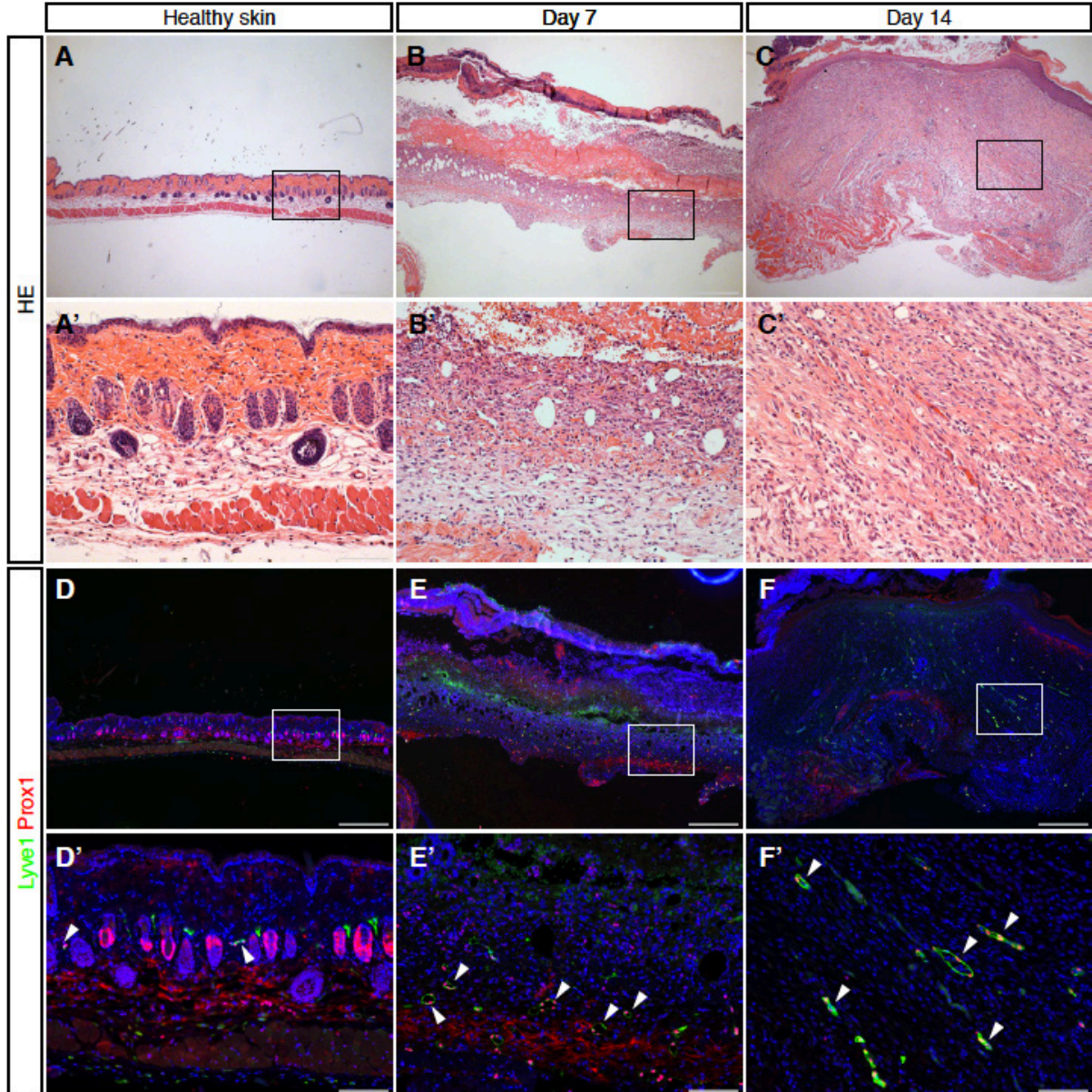
recombination leads to loss of exon 3 and creation of a recombined (RC) *Vegfc* allele (*Vegfc^{RC}*). **(B)** *Vegfc^{RC/RC}* embryos display severe edema (indicated by white arrow) at E15.5 consistent with loss of lymphatic function. **(C and D)** Staining for Lyve1+Prox1+ LECs in E15.5 embryos reveals the loss of both deep lymphatic vessels in the jugular region **(C)** and superficial cutaneous lymphatic vessels **(D)** in *Vegfc^{RC/RC}* embryos. **(E)** qPCR analysis of *Vegfc* transcript levels in mice after tamoxifen treatment of adult animals demonstrates highly efficient recombination of *Vegfc* in all tissues tested. V, vein; A, artery; L, lymphatic vessel. Scale bars = 100 μ m. Error bars indicate SEM.

Supplemental figure 2



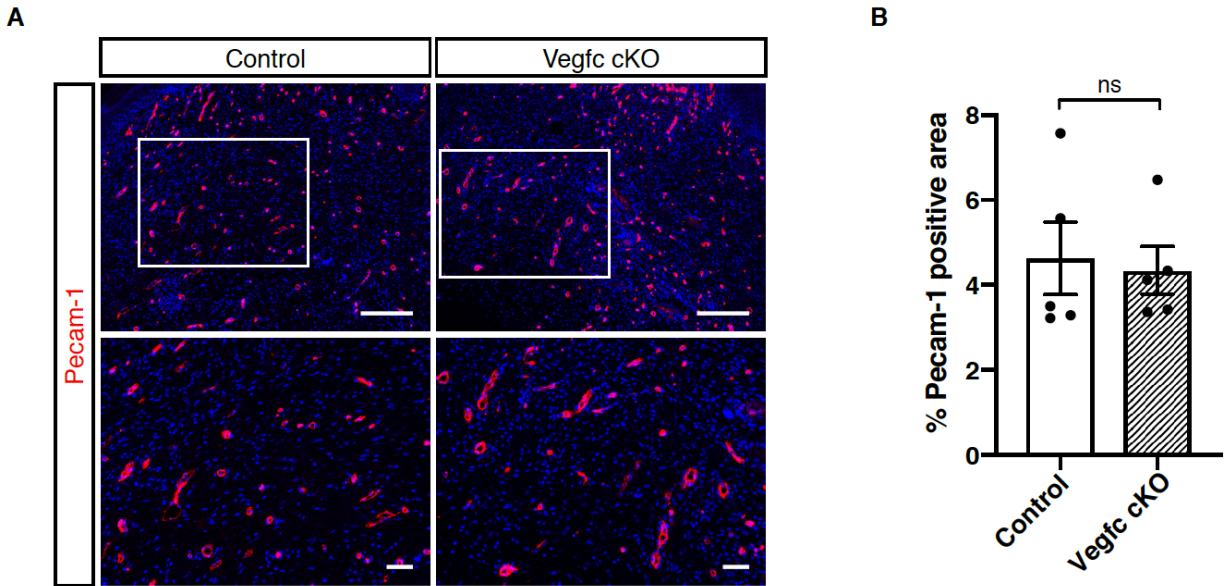
Supplemental figure 2. Mouse tail injury is a platelet-rich wound environment, while the skin injury is largely devoid of blood and platelets. Mice were injected with PeCy7-labeled CD-41 antibodies, given either the tail injury or skin injury, and imaged within the wound site for fluorescently labeled platelets. **(A)** Bright field image of tail injury. **(B)** Lower magnification image of boxed injury site in (A), viewed in the red channel. **(B')** Higher magnification view of boxed inset in (B). White arrows indicate platelet clusters (not all platelet clusters are indicated). **(C)** Bright field image of skin injury. **(D)** Lower magnification image of boxed injury site in (C), viewed in the red channel. **(D')** Higher magnification view of (D) corresponding to boxed inset. Note the lack of bright spots representative of platelet clumps. Scale bars: A = 500 μm , B, D = 100 μm , B', D' = 20 μm , C = 1000 μm .

Supplemental figure 3



Supplemental Figure 3. Characterization of lymphangiogenesis following a full thickness dorsal skin excision wound. (A-C) HE staining of histological sections of healthy skin, granulation tissue, and new skin at the indicated timepoints. (A'-C') Higher magnification images of boxed areas in A-C. (D-F) Immunohistochemical staining for Lyve1+Prox1+ LECs in healthy skin, granulation tissue and new skin. White arrowheads indicate lymphatic vessels containing Lyve1+Prox1+ LECs. Scale bars in A-F = 500 μ m, A'-F' = 100 μ m.

Supplemental figure 4



Supplemental Figure 4. Loss of VEGFC does not affect angiogenesis after skin wounding. (A) Immunostaining of new skin 14 days after wounding shows no major differences in blood vessel density (Pecam-1+ vessels) between control and Vegfc cKO animals. (B) Quantification of blood vessel density by Pecam-1 positive area. Scale bars: top panels in A = 200 μ m; bottom panels = 50 μ m. ns, not significant.

Supplemental Video Legends

Supplemental video 1. Collateral lymphatic capillary flow around injury site. Shown is a lymphangiogram performed on day 12 after injury in which dextran flow can be seen in the superficial lymphatic plexus around but not through the injury site. Injection is on the left and flow is from left to right. The video is accelerated, and the actual timing of the video is indicated on the top left hand corner of the video, in MM:SS format.

Supplemental video 2. Restored collecting vessel flow across injury site. Shown is a lymphangiogram performed on day 12 after injury in which dextran flow can be seen both in the superficial lymphatic plexus around through the injury site (top) and in the deeper collecting lymphatic vessel that runs through the injury site (bottom). Injection is on the left and flow is from left to right. The video is accelerated, and the actual timing of the video is indicated on the top left hand corner of the video, in MM:SS format.